

Ride Comfort Analysis Using Quarter Car Model

S. Hegazy* and A. M. Sharaf†

Abstract: This paper presents a detailed theoretical and experimental investigation for ride comfort evaluation at different vehicle speeds. For the purpose of ride comfort evaluation, a quarter car model with two degrees of freedom has been developed. For realistic investigation, the equivalent characteristics of suspension stiffness and the shock absorber characteristics are calculated and incorporated to simulation. Using available quarter car test rig for single independent front suspension, that embodies sprung mass, unsprung mass, suspension system and tire. An excitation of sinusoidal road profiles with constant amplitude is imposed via eccentric wheel that represents the road profiles. The experimental results of sprung mass and unsprung mass accelerations due to road excitation are measured, recorded and processed. A validation of the theoretical results with experimental results has been carried out at different speeds. Good agreement has been obtained when using the equivalent suspension stiffness and damping coefficient as input parameters to quarter car model representing the independent front suspension.

Keywords: Multi-body dynamics, quarter car, vehicle ride analysis, quarter test rig.

Nomenclature

A	Road displacement due to harmonic motion
c_s, c_t	Damping coefficient of shock absorber and tire; (N.s/m).
c_{eq}	Equivalent damping coefficient of shock absorber
k_s, k_t	Suspension and tire stiffness; respectively (N/m).
k_{eq}	Equivalent spring stiffness, (N/m)
m_s	Sprung mass (kg).
m_u	Unsprung mass in (kg).
t	time
V	Vehicle speed (m /sec)
Z	Amplitude of harmonic motion
λ	Wave length of exciting road profile

Abbreviations

ADAMS	Automatic Dynamic Analysis of Mechanical Systems
DOF	Degree of freedom
RMS	Root Mean Square

* Egyptian Armed Forces, Egypt, shawky26@yahoo.com

† Egyptian Armed Forces, Egypt, al_hossein2005@hotmail.com

1. Introduction

The main functions of the suspension are to provide ride comfort and to maintain tire loadings; safety and stability. The performance of suspension system can be assessed in terms of three parameters, discomfort parameter, suspension working space and dynamic tire load [1]. The discomfort parameter is the sprung mass acceleration transmissibility which is the ratio of sprung mass acceleration to the road excitation. The suspension working space measures the variation of the displacement about its static position while the dynamic tire deflection measures the road holding. A good suspension system should provide small acceleration of the body mass, and a small suspension working space. The ride characteristics are studied using quarter car model. This method has been widely used to investigate the performance of passive, semi-active and fully active suspension systems [2-5]. Non-dimensional vehicle models are used to simulate the vehicle suspension system to study the effect of design parameters on ride comfort and road holding [6]. A considerable research has been conducted to define ride comfort limits [7-9]. They include shake test, ride simulator experiment and roadway at constant speed. The recommended root mean square, for ride quality is 0 - 0.04 g for smooth ride, 0.04 g - 0.06 g for medium ride and above 0.06 g for rough ride [10]. In this paper a quarter car model is developed and experimental setup with required sensors has been established. The theoretical results have been compared with analytical results, good agreements are obtained.

2. Mathematical Model of Quarter Car

The vehicle suspension system is modeled with 2-DOF quarter car model, shown in Fig. 1. The two degrees of freedom are sprung mass, and the unsprung mass displacements. The suspension system and tire are represented by a spring and damper. The equations of motions are:

$$m_s \ddot{z}_1 + c_s (\dot{z}_1 - \dot{z}_2) + k_s (z_1 - z_2) = 0 \quad (1)$$

$$m_u \ddot{z}_2 - c_s (\dot{z}_1 - \dot{z}_2) - k_s (z_1 - z_2) + c_t (\dot{z}_2 - \dot{z}_0) + k_t (z_2 - z_0) = 0 \quad (2)$$

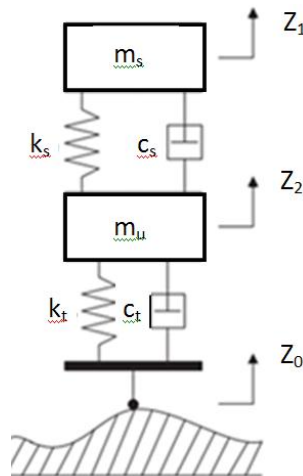


Figure 1 Quarter car model (2-DOF)

Assuming harmonic motion of base and the masses

$$z_i(t) = Z_i e^{j\omega t}, i = 0,1,2$$

$$\dot{z}_i(t) = Z_i j\omega e^{j\omega t} = j\omega Z_i(t)$$

$$\ddot{z}_i(t) = -Z_i \omega^2 e^{j\omega t} = -\omega^2 Z_i(t)$$

where Z_i is the amplitude of harmonic motion

$$\begin{bmatrix} -m_s \omega^2 + k_t + k_s + j\omega(c_t + c_s - k_s - c_s j\omega) \\ -k_s - c_s j\omega \end{bmatrix} \times \begin{bmatrix} Z_2 \\ Z_1 \end{bmatrix} = \begin{bmatrix} (k_t + j\omega c_t) z_0 \\ z \end{bmatrix}$$

The frequency response functions of the two degrees of freedom, for sprung and unsprung masses are investigated in the form of displacement transmissibility. The displacement transmissibility is defined as the ratio of output displacement to the road input excitation.

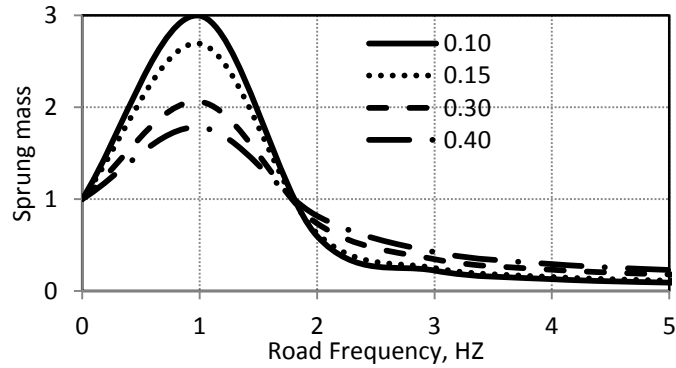
The sprung mass displacement transmissibility:

$$\frac{z_1}{z_0} = \frac{(k_s + j\omega c_s)(k_t + j\omega c_t)}{(-m_u \omega^2 + k_t + k_s + j\omega(c_t + c_s))(-m_s \omega^2 + k_s + c_s j\omega) - (k_s + j\omega c_s)^2} \quad (3)$$

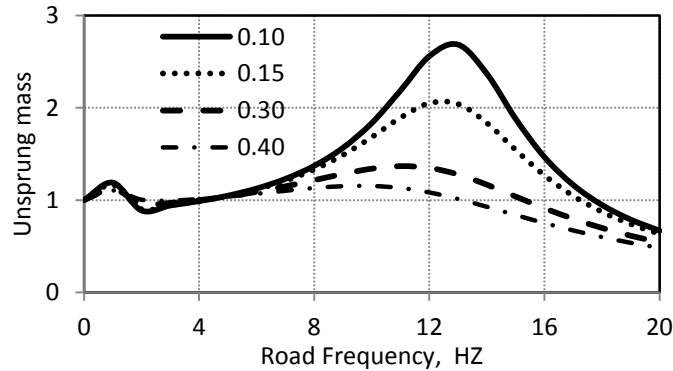
The unsprung mass displacement transmissibility:

$$\frac{z_2}{z_0} = \frac{(-m_s \omega^2 + k_s + j\omega c_s)(k_t + j\omega c_t)}{(-m_u \omega^2 + k_t + k_s + j\omega(c_t + c_s))(-m_s \omega^2 + k_s + c_s j\omega) - (k_s + j\omega c_s)^2} \quad (4)$$

The transmissibilities of the sprung mass (z_1) and unsprung mass (z_2) with respect to the road input excitation are shown in Fig. 2(a) and 2(b) respectively. The effects of damping ratio on transmissibility of sprung and unsprung masses are shown in Fig. 2(a) and 2(b). As the damping ratio is increased, the resonant peaks are attenuated, but isolation is lost both at high frequency and at frequencies between the two natural frequencies of the system. The effects of sprung mass and unsprung mass on transmissibility are shown in Fig. 3(a) and 3(b). As the sprung mass increases, the transmissibility decreases, and vice versa for unsprung mass.



(a) Sprung mass displacement transmissibility



(b) Unsprung mass displacement transmissibility

Figure 2. Displacement transmissibility at different damping ratio

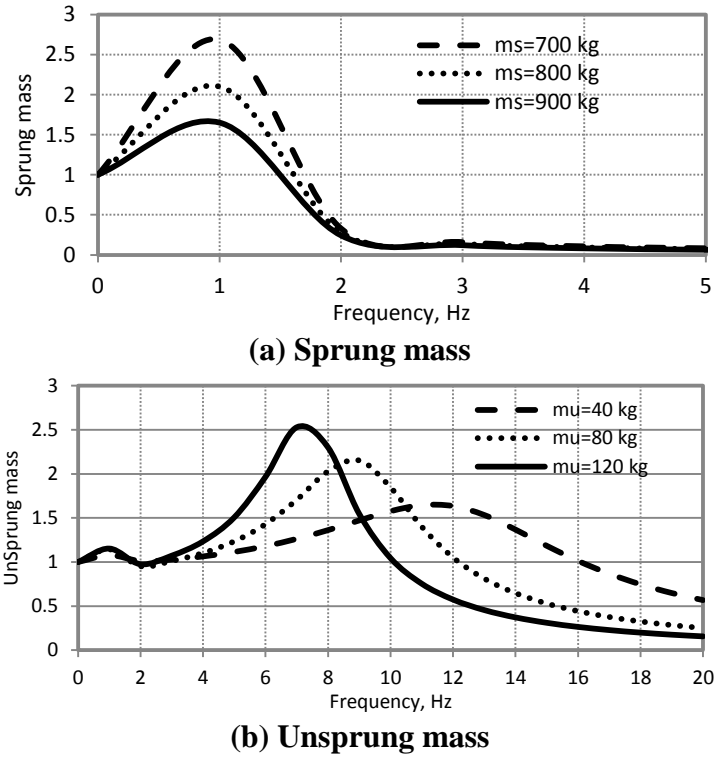


Figure 3. Displacement transmissibility at different mass ratio

3 Equivalent Spring Stiffness and Shock Absorber Coefficient

The suspension stiffness and shock absorber characteristics are obtained experimentally [11]. The equivalent spring stiffness and shock absorber coefficient are calculated based on geometry, shown in Fig. 4. Where the angle $\alpha=5$ deg with the direction of wheel motion and displaced at distance of $b = 390$ mm and $a=270$ mm from the wheel center. So, the equivalent spring stiffness, k_{eq} and shock absorber damping coefficient, c_{eq} based on experimental testing of front suspension parameters ($k = 25000$ N/m), are:

$$c = \left(\frac{a}{b} \cos \alpha\right)^2 = \left(\frac{270}{390} \cos(5)\right)^2 = 0.476 \quad (5)$$

The equivalent stiffness, k_e :

$$k_{eq} = k_s \left(\frac{a}{b} \cos \alpha\right)^2 = 25000 * 0.476 = 11891 \text{ N/m} \quad (6)$$

The equivalent damping coefficients, c_s are calculated based on Table 1 where each value from actual characteristics is multiplied by factor, 0.476. The equivalent values are given in Table 2:

Table 1: Actual damping coefficients

Velocity(mm/s)	-500	-250	-100	0	100	250	500
Soft (N.s/m)	-700	-450	-350	0	150	500	700
Hard (N.s/m)	-900	-650	-350	0	500	1250	1500

Table 2: Equivalent damping coefficients

Velocity(mm/s)	-500	-250	-100	0	100	250	500
Soft (N.s/m)	-333	-214	-143	0	95	238	333
Hard (N.s/m)	-428	-309	-167	0	238	595	714

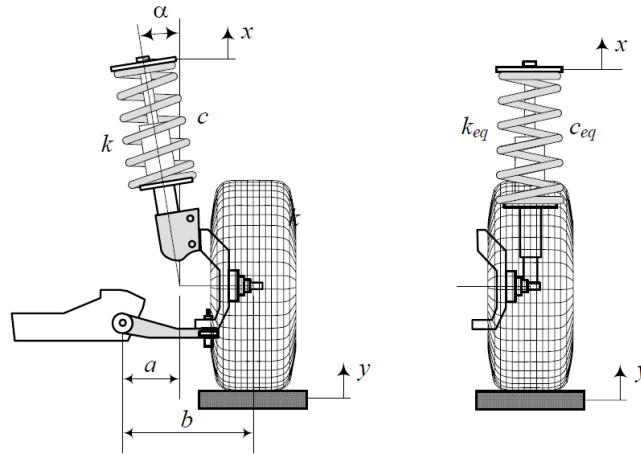


Figure 4 Front independent suspension and its equivalent vibrating model

4. Road Input Profile

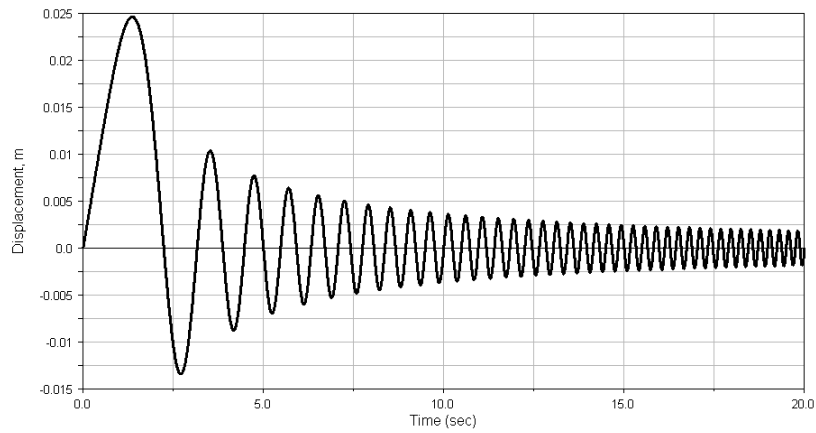
Two road input profiles are considered. The first road is represented by a swept sine wave with decreased amplitude at frequency increased with a constant rate of 0.1 Hz/s, Fig. 5(a). The peak velocity is held constant while the frequency is increased. The second is represented by a sinusoidal wave with constant amplitude with time. The amplitude is 0.025 m, wave length; λ is 1.85 m at different speeds will give different excitation frequencies. Figure 5(b) shows the road inputs at two frequencies (1.38-1.85 Hz). For numerical calculations, the road profiles are simulated numerically using equations 3-4

$$Z_r = \frac{A}{\left(\frac{2\pi \times 0.1 \times t}{\lambda}\right)} \times \sin\left(\frac{2\pi \times 0.1}{\lambda} t\right) t^2 \quad (3)$$

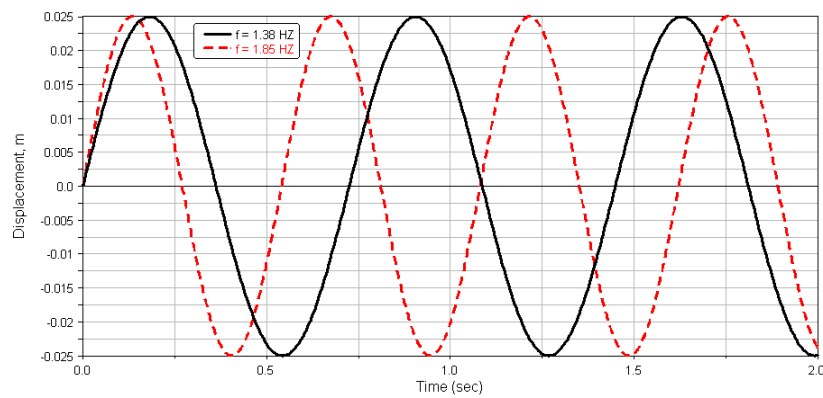
$$Z_r = A \times \sin\left(\frac{2\pi V}{\lambda} t\right) \quad (4)$$

5. Theoretical Analysis and Simulation Studies

Using multi-body dynamics package, ADAMS the theoretical analysis is performed for various road excitations with amplitude 25 mm. The real characteristics of suspension stiffness and shock absorber damping coefficients are measured experimentally [11]. The equivalent suspension stiffness and shock absorber damping coefficient are calculated and introduced to the quarter car model shown in Fig. 6. The model is simulated for 20 sec and 5000 steps at different velocities, varying from 9-35 km/h on road profiles shown in Fig. 5. The needed parameters for mathematical quarter car model are given in Table. 3. The dynamic analysis provides the time history solution for all of the displacements, velocities, accelerations. Selected results based on Fig. 5(a) are presented in Fig. 7-10. Figure 7 shows the variations of sprung mass and unsprung mass displacement with time. It is clear that the displacement of sprung mass decreases and tends to zero at high frequency. Figure 8 shows the variations of suspension working space with time. The root mean square (RMS) to road input is equal to 0.58. Figure 9 shows the variations of sprung and unsprung mass acceleration with time. The RMS of sprung mass acceleration is equal to 0.22 while the RMS for unsprung mass acceleration is equal to 0.42. Figure 10 shows the variations of dynamic tire force with time where the dynamic tire force is the instantaneous tire deflection (difference between road displacement and unsprung mass displacement) and vertical tire stiffness. The RMS is 2775 N.



(a) Swept sine wave with amplitude decreases as a function of the frequency



(b) Sinusoidal road input with constant amplitude at different frequencies

Figure 5 Road input profiles

Table 3: Parameters of quarter car

Parameter	Mathematical	Experimental
Sprung mass	240 kg	240 kg
Unsprung mass	43 kg	43 kg
Spring stiffness	12 kN/m	25 kN/m
Damping coefficient	Table (2)	Table (1)
Tire stiffness	200 kN/m	200 kN/m

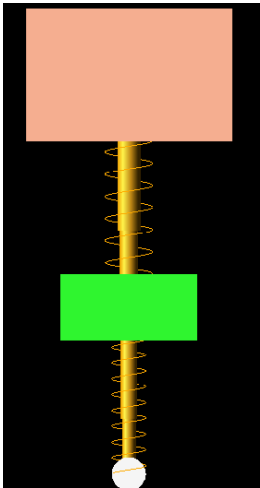


Figure 6 Two DOF quarter car model

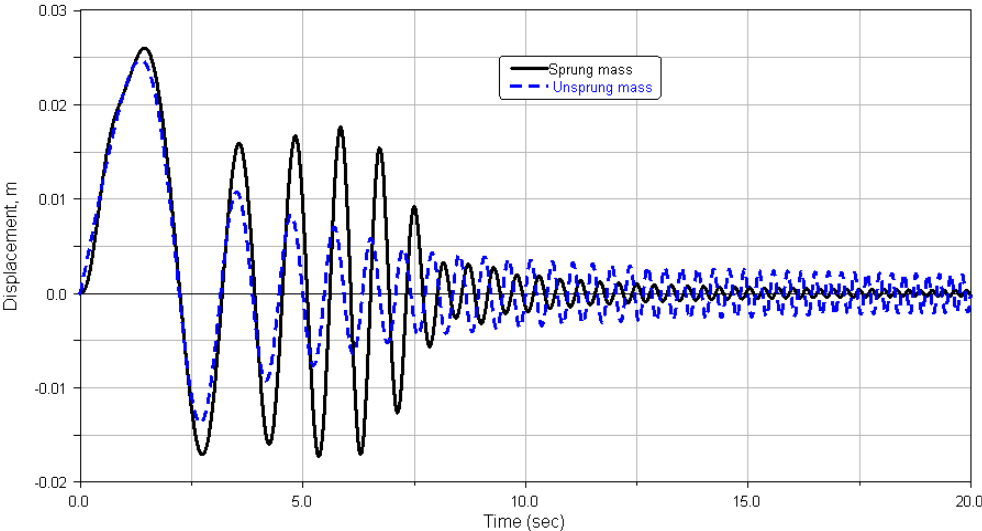


Figure 7 Variation of displacement with time

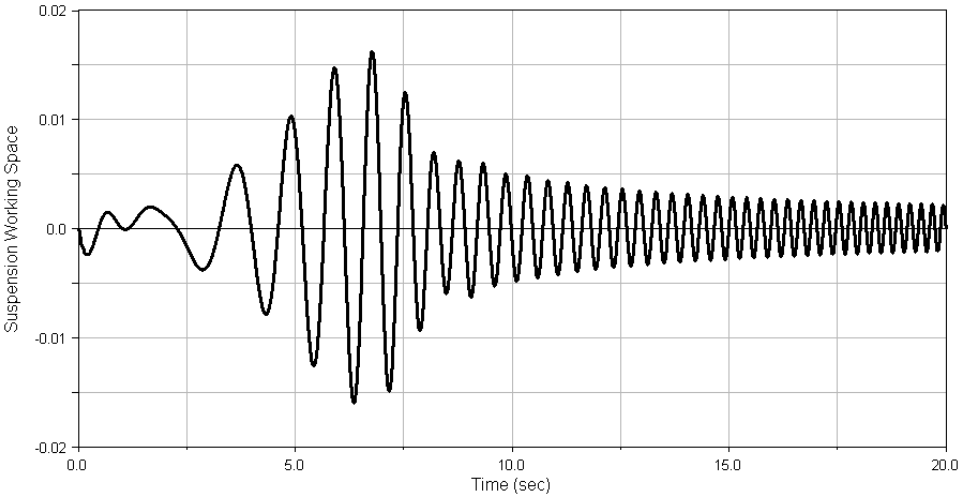


Figure 8 Variation of suspension working space with time

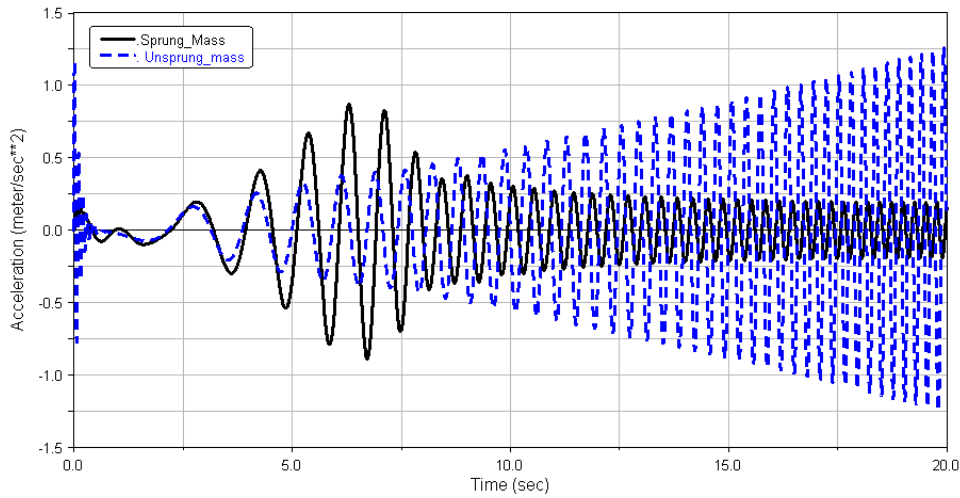


Figure 9 Variation of vertical acceleration with time

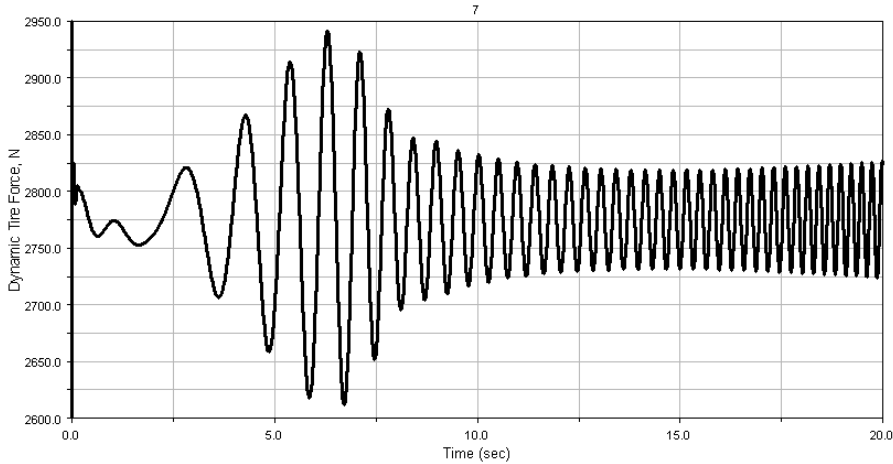


Figure 10 Variation of dynamic tire force with time

6. Validation of the Simulation Results

Using available quarter car test rig for single independent front suspension [11] that embodies sprung mass, unsprung mass, suspension system and tire, shown in Fig. 11. An excitation of sinusoidal road profiles with constant amplitude 25 mm (given in Fig. 5(b)) is imposed via eccentric wheel that represents the road profiles. The experimental results of sprung mass and unsprung mass accelerations due to road excitation are measured, recorded and processed. Selected results are presented graphically, Fig. 12-13 to compare between theoretical and experimental measurements. Figure 12 shows comparisons between theoretical and experimental results of sprung mass accelerations, good agreement has been obtained. In Fig. 12(a) the RMS of experimental sprung mass acceleration is 1.37 corresponding to 1.49 for theoretical calculation and in Fig. 12(b) the RMS of experimental sprung acceleration is 2.15 corresponding to 1.50 for theoretical calculation. These small differences are due to vertical frictions between rollers and frame. In Fig. 13(a) the RMS of experimental unsprung mass acceleration is 1.19 corresponding to 1.29 for theoretical calculation and from Fig. 13(b) the RMS of experimental unsprung mass acceleration is 1.71 corresponding to 2.31 for theoretical calculation. These small differences are due to nonlinear tire stiffness.

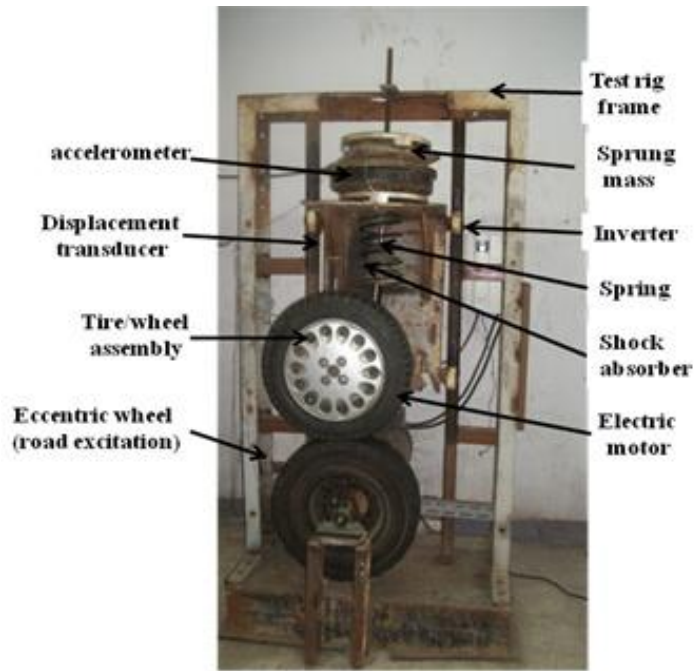
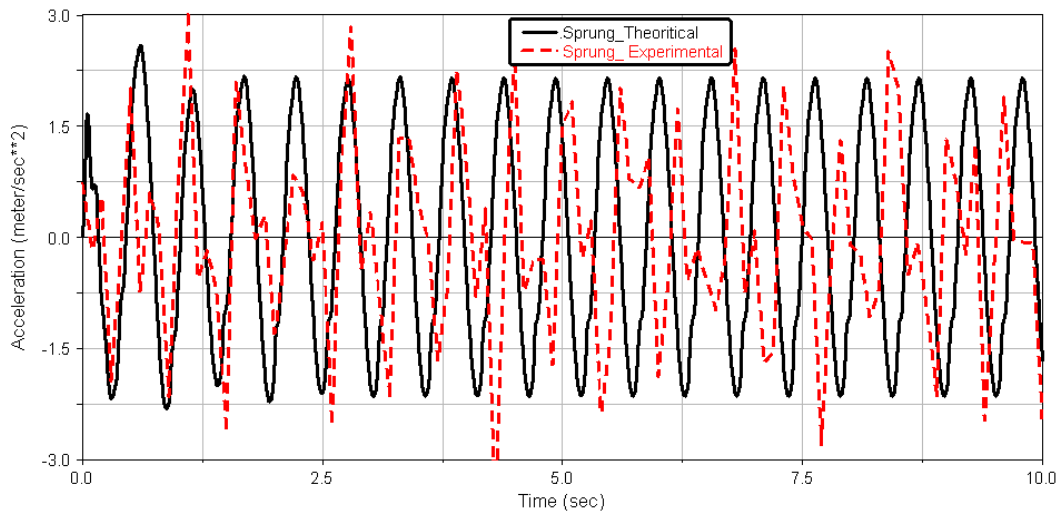
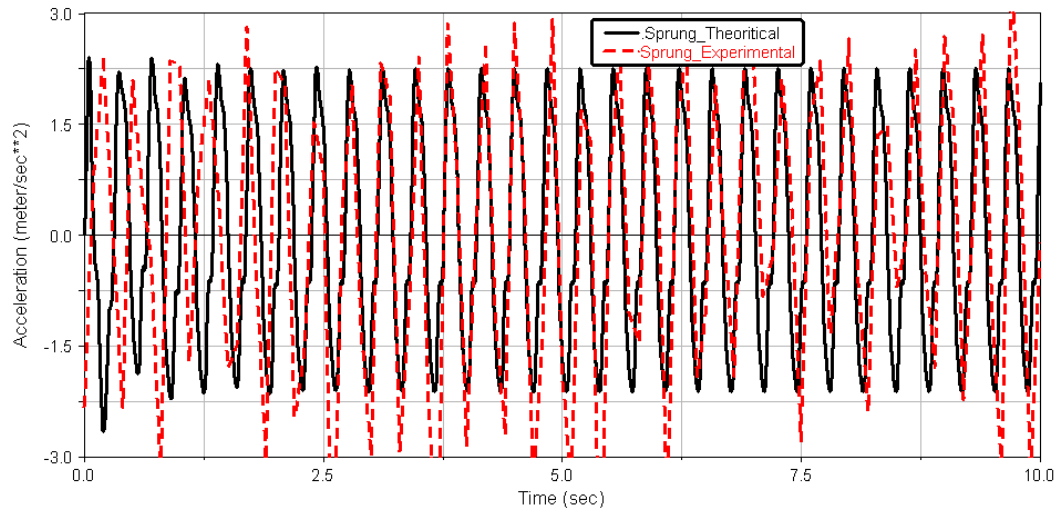


Figure 11 View of quarter car test rig [11]



(a) Sprung mass acceleration at $f=1.85$ Hz



(b) Sprung mass acceleration at $f=2.9$ Hz

Figure 12 Comparisons between theoretical and experimental sprung mass accelerations

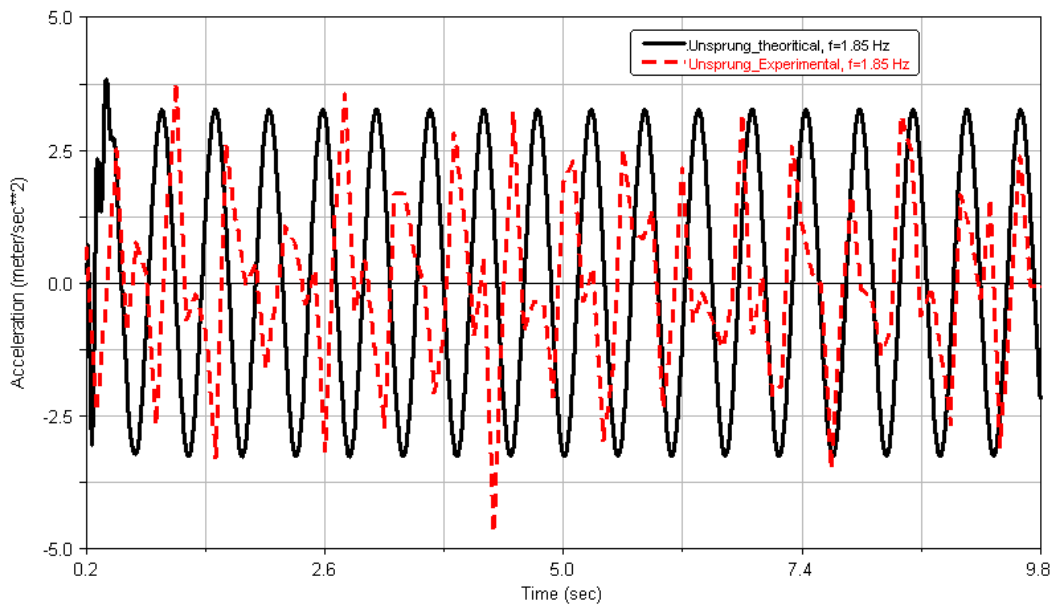
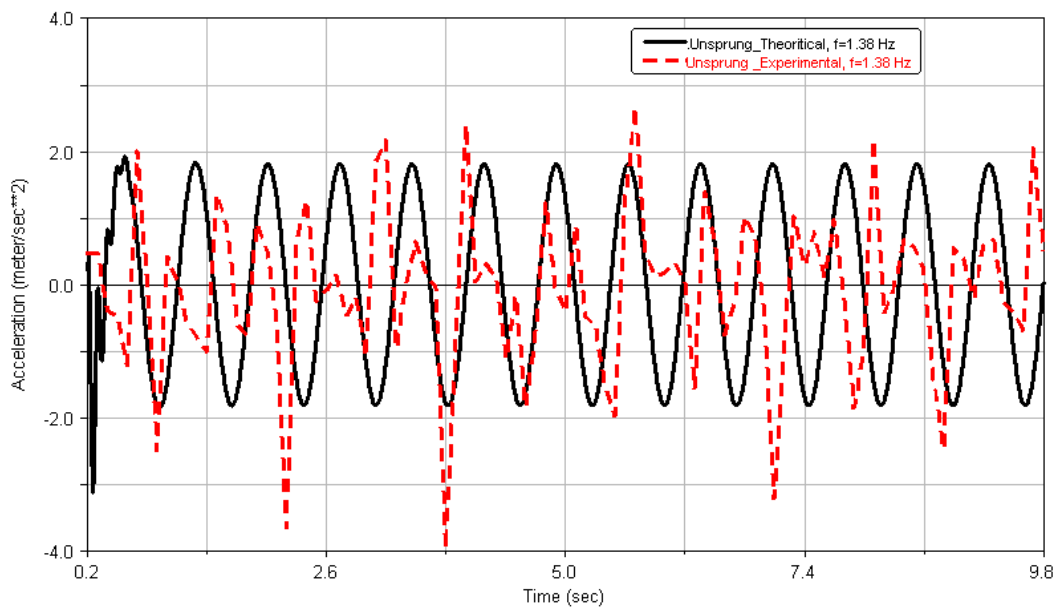
(a) Unsprung mass acceleration at $f=1.38$ Hz(a) Unsprung mass acceleration at $f=1.85$ Hz

Figure 13 Comparisons between theoretical and experimental unsprung mass accelerations

Conclusions

This paper presented a theoretical analysis for ride comfort analysis using quarter car model. For this purpose, an experimental testing has been conducted for suspension parameters in terms of spring stiffness and shock absorber damping force coefficient in two modes; soft and hard. The frequency response functions are investigated in terms of displacement transmissibility for sprung and unsprung masses. The effect of damping ratio, sprung and unsprung mass on transmissibility has been studied. At low damping, the resonant transmissibility is relatively large and vice versa as the damping ratio is increased, the transmissibility ratio will be decreased. As the sprung mass increases, the transmissibility decreases, and vice versa for unsprung mass.

A quarter car model is simulated using multi-body dynamics and the theoretical results are obtained in terms of vertical acceleration, suspension working space and dynamic tire load. Using available quarter car test rig for single independent front suspension, a comparison between theoretical and experimental results for sprung mass and unsprung mass acceleration has been carried out at different speeds for sinusoidal road profile. A good agreement has been obtained and the small differences of sprung mass accelerations are due to vertical frictions between rollers and frame. While the small differences of unsprung mass accelerations are due to nonlinear tire stiffness intended by test rig.

References

- [1] Crolla D.A., Firth G., Horton D. "An Introduction to vehicle dynamics", Automotive Dynamics Engineering Ltd. (Course notes), November, 1992.
- [2] Ahmadian, M., and Pare, K. "A Quarter-Car Experimental Analysis of Alternative Semiactive Control Methods", *J. of Smart Material Systems and Structures*, Vol. 11, No. 8, Aug. 2000, pp. 604 – 612.
- [3] Simon, D.E., and Ahmadian, M. "Vehicle Evaluation of the Performance of Magneto Rheological Dampers for Heavy Truck Suspensions", *ASME J. of Vibration and Acoustics*, Vol. 123, No. 3, July 2001, pp. 365 – 375.
- [4] Simon, D.E., and Ahmadian, M. "An Alternative Semiactive Control Method for Sport Utility Vehicles," *J. of Automobile Engineering*, Vol. 216, Part D, April 2002, pp. 125 – 139.
- [5] Cebon, D., Besinger, F. H., and Cole, D. J., "Control strategies for semiactive lorry suspensions", *Proc .Inst. Mech. Engrs, Part D: J. Automobile Engineering*, 1996, 210, 161–178.
- [6] Hegazy, S. and Sandu, C., "Vehicle Ride Comfort and Stability Performance Evaluation," *SAE Technical Paper 2009-01-2859*, 2009, doi:10.4271/2009-01-2859
- [7] Sharp, R. S. and Hassan, S. A., "Evaluation of passive Automotive suspension systems with variable stiffness and damping parameters", *Vehicle System Dynamics*, 1986, 15(6), 335–350.
- [8] Krtolica, R., & Hrovat, D., "Optimal active suspension control based on a half car model", *Proceedings of the 29th IEEE of the conference on decision and control*. Honalulu, Hawaii, 1990, pp. 2238–2243.
- [9] Hegazy S. "Modeling and Simulation of Tracked Vehicles for Pitch, Bounce and Roll", 11th International Conference on Applied Mechanics and Mechanical Engineering, MTC, Cairo, Egypt, 2004.
- [10] Pinhas, B., "Magic Numbers in design of suspensions for passenger cars", *SAE paper No. 911921*, 1991
- [11] M. Ajaj, "Study of Vehicle Suspension Design for Ride Comfort", *Ph. D. Thesis, MTC*, 2011